Mirror effect at the Brewster angle in semiconductor rectangular gratings

L. Pilozzi and A. D'Andrea
Istituto di Metodologie Avanzate Inorganiche, CNR, box 10-I-00016 Monterotondo Scalo, Roma, Italy

H. Fenniche
Faculté des Sciences de Tunis, Campus Universitaire, 1060 Tunis, Tunisie

(Received 10 November 2000; revised manuscript received 23 March 2001; published 27 November 2001)

The Green's functions of microstructured rectangular gratings, and the electric field for a nonlocal susceptibility are given in explicit form. A very broad energy band with reflectivity of almost 1 is shown by model calculation for a strongly diffractive grating when the angle of incidence of the light is very close to the Brewster angle of the equivalent slab, and the grating thickness is about one light wavelength. The physical origin of this interesting effect is completely explained as an interplay between grating resonances and surface waves. In the energy range from infrared to ultraviolet, the ratio between bandwidth ΔE and band-edge energy E_0 scales as $\Delta E/E_0 = L_x/d$, where L_x is the lateral dimension, and d is the periodicity of the grating. The easy tailoring of this effect should be promising for optoelectronic and photonic large-band device applications.

DOI: 10.1103/PhysRevB.64.235319 PACS number(s): 78.20.Bh, 78.66.−w, 85.35.Be

I. INTRODUCTION

The optical properties of the gratings were intensively studied at the very beginning of the diffractive optics.[1] More recently, papers devoted to the optical response in dielectric gratings show an increasing presence in the literature (see Refs. 2–12 and references therein) due to the improvement in nanotechnology manipulation. This has allowed one to obtain rectangular gratings where the periodicity is of the order of the light wavelength in the visible range of energy, and the lateral dimension of the optically active material is close to the Bohr radius of Wannier exciton. These properties permit the study of new fundamental effects due both to the electric charges (electron-hole, exciton) and to the electric field confinements that are promising for optical device applications.

The resonant diffractive phenomena in gratings have been investigated starting from the pioneering paper of Wood[1] (Wood's anomalies). Popov, Mashev, and Maystre[2] have studied a resonant grating waveguide structure by a phenomenological model, and Wang *et al.*[3] have explained this effect by a rigorous numerical calculation. That calculation shows a maximum (resonance) in the zero-order reflectance spectrum when a guided mode is excited in the system. These resonances were also studied by the present authors in Ref. 4 exactly solving the Maxwell's equations, while Rosenblatt, Sharon, and Friesem have summarized this effect in a review paper,[5] and, moreover, it has been recently proposed to be well suited for the optical spectral filter realization.[6]

Optical emission in quantum wells and in quantum-well wires induced by rectangular grating coupler was experimentally studied by Kohl *et al.*,[7,8] and a large polarization anisotropy was pointed out by the same authors. The electromagnetic origin of this phenomenon, at variance with heavy-hole–light-hole interaction in quantum wires,[9] was accounted for by the present authors[10,11] by computing the contribution of local field, and the numerical results compare well with the experiment. Moreover, the same systems were also studied in a subsequent paper by Ils *et al.*,[12] and the electromagnetic origin of this anisotropy was confirmed. Finally, the grating-coupler-induced absorption in a quantum well under resonant condition was studied by the authors,[13] and the anomalous behavior of the exciton absorbance for high parallel wave vector was computed by selected numerical examples.

Grating-induced distortion in the exciton-polariton absorbance in a planar laser cavity was studied by Kavokin, Kliteevski, and Vladimirova[14] and by Pilozzi and D'Andrea.[13] In the latter paper, a very large Rabi splitting (about 25 meV for a GaAs cavity) was obtained by model calculation extending dramatically the possibility of performing the radiation-matter interaction tailoring in these systems.

The aim of the present work is twofold, namely, (i) to explain by model calculation the physical origin of the broad reflection band (mirror effect) in strongly diffractive dielectric gratings. The easy tailoring of this interesting phenomenon, and its promising device applications will be also briefly discussed, and (ii) to give the general form of the Green's functions for computing exciton polaritons in a semiconductor grating of quantum-well wires in semiclassical framework and in effective-mass approximation; this formulation is well suited also for computing the optical response in semi-infinite photonic crystals.

It is well known that the local electric field in a grating can be computed by solving Maxwell's equations by using an expansion in a rather large base of plane waves, where the evanescent waves take a crucial role. On the other hand, for computing the optical response, and in general for the asymptotic optical properties, a rather small number of interacting waves (usually traveling and guided) are sufficient for obtaining the numerical convergence, and the higher-order evanescent components usually give negligible contribution.[5,14] In the present calculation, the optical response of the grating, computed at the Brewster angle of the equivalent slab, is to our knowledge the first case where the former approximation gives completely wrong physical results.

Finally, the role of disorder in the optical response will be taken into account in the model calculation. In fact, the full

coherence in space and time of the exciton-polariton is usually an implied assumption in the optical response calculation, and the in-plane wave-vector conservation is generally assumed when the interface boundary conditions are imposed. This condition is not fully met in real systems.[15,16] In fact, alloy disorder, phonon scattering, and interface roughness are dephasing mechanisms that can broaden the absorbance peaks and destroy the coherence of the optical response, especially when guided wave and the multireflection mechanism are involved.[16] Moreover, for electromagnetic modes with high parallel-wave-vector values generated by a dielectric grating, also *e-h* mass nonparabolicity must be taken into account.[15] In conclusion, negligible dephasing and parabolic *e-h* effective masses are two largely used conditions that should be carefully checked by comparison with experimental results.

II. THEORY

Let us consider a planar dielectric grating of quantum wires as shown in Fig. 1 where the wires are along the *y* axis. The grating has periodicity d, lateral dimension L_x, and dielectric constant ε_b, while its thickness value is L_z. We consider an incident plane wave from the vacuum side ($z<0$) of frequency ω, and in-plane wave-vector component $k_\parallel = k_x = \omega \sin(\vartheta_i)/c$, where ϑ_i is the angle of incidence ($k_y=0$).

The grating of quantum well wires is placed between two semi-infinite spaces (vacuum for $z<0$ and $z>L_z$) and its total polarization is

$$\vec{P}(x,\ z)=\vec{P}^{(1)}(x,\ z)+\vec{P}^{(2)}(x,\ z), \tag{1}$$

where $\vec{P}^{(1)}(x,z)$ is the polarization due to the background dielectric function modulation, and $\vec{P}^{(2)}(x,z)$ is the exciton polarization confined in the rectangular wires. The polarization of the local dielectric grating and the nonlocal polarization of Wannier exciton are given in Ref. 4 and Ref. 10, respectively for $L_z \ll a_B \ll L_x$, where a_B is the Bohr exciton radius.

The total polarization in mixed coordinates (k_x, z) is

$$\vec{P}(k_x+G,z)=\vec{P}^{(1)}(k_x+G,z)+\vec{P}^{(2)}(k_x+G,z), \tag{2}$$

where the reciprocal lattice vector is $G=2\pi l/d$ with $l=0, \pm 1, \pm 2, \ldots, \pm N$, and $N\to\infty$. The dielectric grating polarization is

$$\vec{P}^{(1)}(k_x+G,z)\equiv \frac{1}{4\pi}\sum_{G'} [\varepsilon_{G,G'}-\delta_{G,G'},\varepsilon_0]\vec{E}(k_x+G',z), \tag{3}$$

where the dielectric tensor of the grating $\epsilon_{G,G'}$ is given by

$$\varepsilon_{G,G'}=\varepsilon_0\delta_{G,G'}+\frac{2}{d}\Delta\varepsilon\,\frac{\sin[(G-G')L_x/2]}{G-G'}, \tag{4}$$

where $\varepsilon_0=1$ is the vacuum dielectric constant and $\Delta\varepsilon=\varepsilon_b-\varepsilon_0$ is the dielectric contrast. The averaged dielectric constant $\overline{\varepsilon}$, that describe the so called ''equivalent slab model,'' is

$$\overline{\varepsilon}=\varepsilon_b L_x/d+\varepsilon_0(1-L_x/d), \tag{5}$$

and is equal to the diagonal matrix elements of the dielectric tensor of Eq. (4). The exciton nonlocal polarization is

$$\vec{P}^{(2)}(k_x+G,z)=\sum_{G'}\int dz'\,\vec{\vec{\chi}}(k_x+G,k_x+G',z,z')\times\vec{E}(k_x+G',z'),$$

where $\vec{\vec{\chi}}(k_x+G,k_x+G',z,z')$ is the susceptibility tensor. It is well known that for Wannier exciton in a wire, the susceptibility is the degenerate kernel of the integral equation derived from the Maxwell's equations, and it is[10]

$$\vec{P}^{(2)}(k_x+G,z)=\sum_{i,j}\frac{S_0(\omega)}{E_{ij}(k_Y)-\hbar\omega-i\Gamma_{\rm NR}(\omega)}\times\Psi^*_{ij}(\mathbf{r}=0;k_x+G,z)\sum_{G'}\int_0^{L_z}dz'\times\Psi_{ij}(\mathbf{r}=0;k_x+G',z')\vec{E}(k_x+G',z'), \tag{6}$$

where $\Psi_{ij}(\vec{r}=0;k_x+G,z)$ is the Fourier transform of the Wannier exciton envelope function computed at $\vec{r}=0$, $E_{ij}(k_Y)=E_{\rm gap}-R^*_{ij}+(\hbar^2/2M)k_Y^2$ is the exciton energy, where R^*_{ij} is the exciton eigenvalue for i and j quantum numbers along x and z directions, k_Y is the center-of-mass wave vector, and $\Gamma_{\rm NR}(\omega)$ is the nonradiative broadening; S_0 is proportional to the square matrix element of the electric dipole operator.[10]

The transformed Maxwell's equations for S and P polarizations ($k_y=0$) are

$$\frac{\partial^2 E_y(k_x+G,z)}{\partial z^2}+\sum_{G'}K_z^{(2)}(G,G')E_y(k_x+G',z)=-4\pi\frac{\omega^2}{c^2}P_y^{(2)}(k_x+G,z) \tag{7a}$$

$$\begin{cases} \dfrac{\partial^2 E_x(k_x+G,z)}{\partial z^2} - i(k_x+G)\dfrac{\partial E_z(k_x+G,z)}{\partial z} \\ \quad + \dfrac{\omega^2}{c^2}\sum\limits_{G'} \varepsilon_{GG'} E_x(k_x+G',z) = -4\pi\dfrac{\omega^2}{c^2} P_x^{(2)}(k_x+G,z) \qquad (7b) \\ -i(k_x+G)\dfrac{\partial E_x(k_x+G,z)}{\partial z} + \sum\limits_{G'} K_z^{(2)}(G,G') E_z(k_x+G',z) \\ \quad = -4\pi\dfrac{\omega^2}{c^2} P_z^{(2)}(k_x+G,z), \qquad (7c) \end{cases}$$

where

$$K_z^{(2)}(G,G') = \frac{\omega^2}{c^2}\varepsilon_{GG'} - (k_x+G')^2\delta_{G,G'}. \qquad (8)$$

The solution of the Maxwell's equation in mixed coordinates [Eqs. (7a)–(7c)] proceeds as in Ref. 11 by solving the Green's function equations respectively for *S* polarization,

$$\frac{\partial^2 G_{yy}(k_x+G;z,z')}{\partial z^2} + \sum_{G'} K_z^{(2)}(G,G') G_{yy}(k_x+G';z,z') = \delta(z-z'), \qquad (9a)$$

and *P* polarization,

$$\frac{\partial^2 G_{xx}(k_x+G,z,z')}{\partial z^2} + \frac{\omega^2}{c^2}\sum_{G'} \varepsilon_{GG'} G_{xx}(k_x+G',z,z') - i(k_x+G)\frac{\partial G_{zx}(k_x+G,z,z')}{\partial z} = \delta(z-z') \qquad (9b)$$

$$-i(k_x+G)\frac{\partial G_{xx}(k_x+G,z,z')}{\partial z} + \sum_{G'} K_{GG'}^{(2)} G_{zx}(k_x+G',z,z') = 0. \qquad (9c)$$

Notice that the other two components of the Green's function tensor, namely, $G_{xz}(k_x+G;z,z')$ and $G_{zz}(k_x+G;z,z')$, can be computed from $G_{xx}(k_x+G;z,z')$ and $G_{zx}(k_x+G;z,z')$ as shown in Ref. 11.

For *S* polarization, let us consider Eq. (9a) in the $(2N+1)\times(2N+1)$ matrix form

$$\frac{\partial^2 \vec{G}_{yy}(z,z')}{\partial z^2} + \vec{\vec{K}}_z^{(2)}\vec{G}_{yy}(z,z') = \vec{\delta}(z-z'), \qquad (10)$$

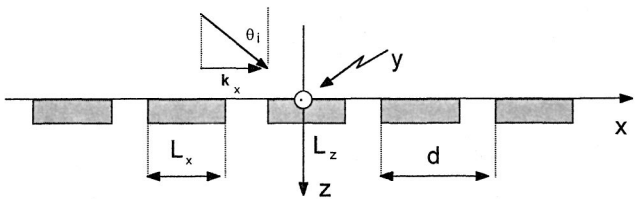

FIG. 1. Self-sustained rectangular dielectric grating of *d* periodicity, L_x lateral dimension, and L_z thickness.

where $\vec{\delta}(z-z')$ is a vector whose *G* components are Dirac's functions $\delta(z-z')$. The unitary matrix that solves the eigenvalue problem

$$\vec{\vec{K}}_z^{(2)}\vec{E}_n = k_n^2\vec{E}_n, \qquad (11)$$

where $n=0,1,...,2N$ is $\vec{\vec{U}} \equiv \{U_{G,n}\} = \{E_n(G)\}$, and its Hermitian conjugate is $\vec{\vec{U}}^+ \equiv \{U_{n,G}^*\}$.

Applying the former unitary matrix to Eq. (10), the transformed equation becomes

$$\frac{\partial^2 \tilde{G}_{yy}(k_n;z,z')}{\partial z^2} + k_n^2\tilde{G}_{yy}(k_n;z,z') = \delta(z-z')\sum_{G'} E_n^*(G'),$$

where, $\vec{\tilde{G}}_{yy}(z,z') = \vec{\vec{U}}^+\vec{G}_{yy}(z,z')$. Finally, by defining the new transformed Green's function, $\tilde{\tilde{G}}_{yy}(k_n;z,z') = \tilde{G}_{yy}(k_n;z,z')/\Sigma_G E_n^*(G')$, we obtain

$$\frac{\partial^2 \tilde{\tilde{G}}_{yy}(k_n;z,z')}{\partial z^2} + k_n^2\tilde{\tilde{G}}_{yy}(k_n;z,z') = \delta(z-z'). \qquad (12)$$

The solution of this kind of differential equation is given in Ref. 17 by Bagchi, Barrera, and Rajagopal:

$$\tilde{\tilde{G}}_{yy}(k_n;z,z') = \frac{1}{2ik_n}[\theta(z-z')e^{ik_n(z-z')} + \theta(z'-z)e^{-ik_n(z-z')}]. \qquad (13)$$

For *P* polarization the algebra is a bit more involved. From Eq. (9c), we obtain

$$G_{zx}(k_x+G;z,z') = i\sum_{G'} (\vec{\vec{K}}^{(2)})_{G,G'}^{-1}(k_x+G')\times\frac{\partial G_{xx}(k_x+G';z,z')}{\partial z}.$$

Substituting this equation in Eq. (9b), one finds

$$\vec{\vec{R}}\frac{\partial^2 \vec{G}_{xx}(z,z')}{\partial z^2} + \frac{\omega^2}{c^2}\vec{\vec{\varepsilon}}\vec{G}_{xx}(z,z') = \vec{\delta}(z-z'), \qquad (14)$$

where

$$R_{GG'} = \delta_{GG'} + (k_x+G)(\vec{\vec{K}}^{(2)})_{GG'}^{-1}(k_x+G').$$

Now, this equation can be solved in the following two steps (i) We solve the following eigenvalue problem:

$$\frac{\omega^2}{c^2}\vec{\vec{\varepsilon}}\vec{\mathbf{E}}_l=\lambda_l\vec{\mathbf{E}}_l, \tag{15}$$

and multiplying Eq. (14) by the Hermitian conjugate of the unitary matrix of the eigenvectors $\vec{\vec{U}}=\{U_{G,l}\}=\{E_l(G)\}$, we obtain

$$\sum_{ll'}\tilde{R}_{ll'}\frac{\partial^2\tilde{G}_{xx}(\lambda_{l'};z,z')}{\partial z^2}+\lambda_l\tilde{G}_{xx}(\lambda_l;z,z')$$

$$=\delta(z-z')\sum_{G'}E_l^*(G'),$$

where, $\tilde{\vec{\vec{G}}}_{xx}(z,z')=\vec{\vec{U}}^+\vec{G}_{xx}(z,z')$, and $\tilde{\vec{\vec{R}}}=\vec{\vec{U}}^+\vec{\vec{R}}\vec{\vec{U}}$. Moreover, by applying the diagonal matrix of the square-roots of the eigenvalues $\vec{\vec{\lambda}}^{-1/2}$, we have

$$\sum_{ll'}S_{ll'}\frac{\partial^2\mathcal{G}_{xx}(\lambda_l;z,z')}{\partial z^2}+\mathcal{G}_{xx}(\lambda_l;z,z')$$

$$=\delta(z-z')\sum_{G'}E_l^*(G')/\lambda_l^{1/2},$$

where $\vec{\vec{S}}=\vec{\vec{\lambda}}^{-1/2}\tilde{\vec{\vec{R}}}\vec{\vec{\lambda}}^{-1/2}$ and $\vec{\mathcal{G}}_{xx}(z,z')=\vec{\vec{\lambda}}^{1/2}\tilde{\vec{\vec{G}}}_{xx}(z,z')$.
(ii) In the second step, we solve the eigenvalue equation for the $\vec{\vec{S}}$ matrix

$$\vec{\vec{S}}\vec{\psi}_n=\frac{1}{k_n^2}\vec{\psi}_n, \tag{16}$$

and applying the Hermitian conjugate of the matrix of the eigenvectors $\vec{\vec{V}}=\{V_{l,n}\}=\{\varphi_n(l)\}$, we obtain the differential equation

$$\frac{1}{k_n^2}\frac{\partial^2\tilde{\mathcal{G}}_{xx}(k_n;z,z')}{\partial z^2}+\tilde{\mathcal{G}}_{xx}(k_n;z,z')=\delta(z-z')\tilde{V}_n,$$

where $\tilde{\vec{\mathcal{G}}}_{xx}(z,z')=\vec{\vec{V}}^+\vec{\mathcal{G}}_{xx}(z,z')$ and

$$\tilde{V}_n=\sum_{l,G}\varphi_n^*(l)E_l^*(G)/\lambda_l^{1/2}.$$

Taking the new Green's function: $\tilde{\tilde{G}}_{xx}(k_n;z,z')=\tilde{\mathcal{G}}_{xx}(k_n;z,z')/\tilde{V}_nk_n^2$, we have the final form,

$$\frac{\partial^2\tilde{\tilde{G}}_{xx}(k_n;z,z')}{\partial z^2}+k_n^2\tilde{\tilde{G}}_{xx}(k_n;z,z')=\delta(z-z'). \tag{17}$$

Notice that Eq. (17) is formally similar to Eq. (12) for *S* polarization and has the same solution.

Finally, knowing the components of the Green's function tensor, the electric field of the grating of quantum-well wires can be written in the integral form

$$E_\alpha(k_x+G;z)=E_\alpha^0(k_x+G;z)+\frac{1}{d}\sum_\beta\left\{\sum_{i,j}\frac{S_0(\omega)}{E_{ij}(k_y)-\hbar\omega-i\Gamma_{\mathrm{NR}}}\int_0^{L_z}dz''\,G_{\alpha\beta}(k_x+G;z,z'')\Psi_{ij}^*(\mathbf{r}=0;k_x+G,z'')\right.$$

$$\left.\times\sum_{G'}\int_0^{L_z}dz'\,\Psi_{ij}(\vec{\mathbf{r}}=0;k_x+G',z')E_\beta(k_x+G',z')\right\}, \tag{18}$$

where $\alpha,\beta=x,y,z$.

The unperturbed electric field components for $\alpha=x,y,z$ [see Eqs. (13) and (18) in Ref. 4] are

$$E_\alpha^0(k_x+G,z)=\sum_n\left[A_ne^{ikn^z}+B_ne^{-ik_nz}\right]E_n^0(k_x+G). \tag{19}$$

Notice that the half width at half maximum of the computed absorbance spectrum embodies also the radiative broadening due to the polaritonic radiation-matter self-energy.[10] Moreover, the formula of Eqs. (1)–(19) allow one to compute the optical response of semi-infinite two-dimensional photonic crystals showing periodicity along *x*, and applying the periodic boundary conditions along *z* direction. The optical response calculation in a two-dimensional semi-infinite photonic crystal by taking into account both the dispersive and the absorbent part of the exciton susceptibility in order to study the role of the electromagnetic surface states is now in progress.

III. RESULTS AND DISCUSSION

It is well known that the reflectivity in a dielectric slab as a function of the incidence angle of the light is very sensitive to the polarization. In fact, while for *S* polarization it shows a monotonic behavior, for *P* polarization it goes to zero at the Brewster angle, where all the light intensity is transmitted. The same behavior is also observed in thin dielectric gratings in the range of energy where only the zero-order diffraction ray ($G=0$) is propagating in the structure, while rather dif-

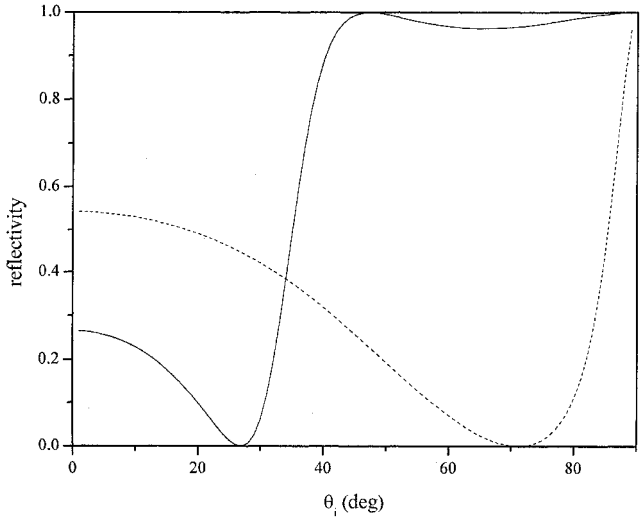

FIG. 2. Reflectivity computed for *P* polarization as a function of the angle of incidence on the surface of the self-sustained rectangular dielectric grating (solid curve), and of an equivalent homogeneous slab (dashed curve). The parameter values are given in the text.

ferent behavior is observed for thick gratings. In fact, let us consider a high diffractive rectangular grating (see Fig. 1) with refractive indices $n_b=\sqrt{\varepsilon_b}=3.34$, $n_0=1$, periodicity $d=300\,\mathrm{nm}$, lateral dimension $L_x=3/4d$, and thickness $L_z=350\,\mathrm{nm}$. The reflectivity for $\vec{\mathbf{P}}^{(2)}(x,z)\rightarrow 0$ is computed by solving the eigenvalue problem of Eqs. (11) and (16) for *S* and *P* polarization, respectively. The reflectivity of the grating for *P* polarization and incident photon energy $\hbar\omega=1.4\,\mathrm{eV}$ is shown in Fig. 2 as a function of the angle of incidence ϑ_i. The results for the equivalent slab approximation shown in the same picture are computed by taking into account the average dielectric constant value of the grating $\overline{\varepsilon}=8.617$. The reflectivity vanishes for the angle of incidence $\vartheta_i=28°$ that is lower than the equivalent slab value ($\vartheta_i=70°$ Brewster angle). Moreover, the reflectivity is nearly one for a very large range of ϑ_i values ($45°<\vartheta_i<75°$).

Now, let us consider the reflectivity for the angle of incidence ($\vartheta_i=60°$) very close to the Brewster angle of the equivalent slab. The results of the calculation are shown in Figs. 3(a) and 3(b) for *S* and *P* polarization, respectively, and the reflectivity of the equivalent slab, and of the lowest diffraction waves ($N=1$) with parallel wave vectors: $q_x=(\omega/c)\sin\vartheta_i$; q_x-G and q_x+G are also shown.

For *S* polarization [see Fig. 3(a)], Fabry-Perot oscillations of the equivalent slab are present at low photon energies, while very complicated oscillations due to the interference of two or more waves propagating in the structure are shown at high energies. For *P* polarization [see Fig. 3(b)], a rather small reflectivity is observed at low energy, while a broadband with the reflectivity almost 1 [$|r_p(\omega)|^2\geqslant 0.97$] is shown at the high energy side of the spectrum.

In order to go a bit deeper in the explanation of this polarization-dependent optical response, let us compute the dispersion curves of the three lowest energy diffraction

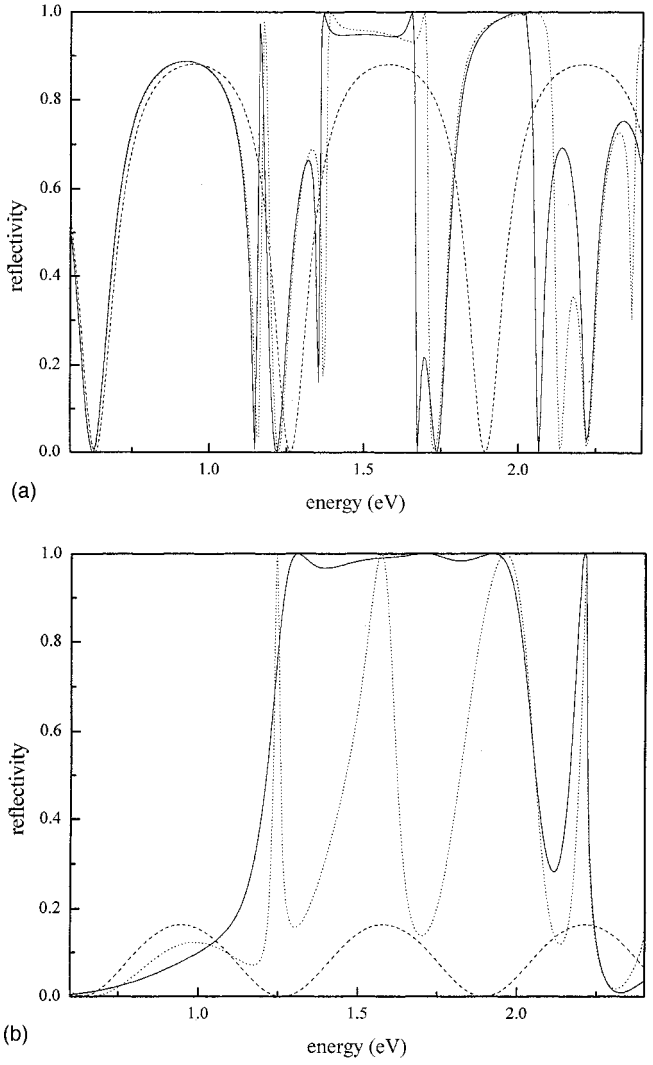

FIG. 3. Reflectivity computed for a self-sustained rectangular dielectric grating for incident angle 60° (solid line) for (a) *S* polarization, and (b) *P* polarization. Reflectivity of the equivalent slab approximation (dashed lines), and for the three lowest-energy waves of the grating (dotted lines) are also reported. The parameter values are given in the text.

waves. The results are presented in Figs. 4(a) and 4(b) for *S* and *P* polarization, respectively. The lowest-energy curve ($n=0$) shows no energy gap, and its behavior is very close to the equivalent slab dispersion, while the higher-energy curves ($n>0$) show threshold energies ($E_{n>0}$) different from zero, such that for photon energy greater than the *n*th threshold energy ($\hbar\omega>E_{n>0}$) the corresponding *n*th evanescent wave becomes propagating in the grating. Therefore, from Fig. 3(a), we notice that for *S* polarization and photon energies lower than $E_1=1.1\,\mathrm{eV}$ the reflectivity shows the usual Fabry-Perot oscillations in a slab, while at higher energies the interference between two propagating waves gives the so-called Wood's resonances [where $|r_s(\omega)|^2=1$] whose reflectivity peaks are superimposed on the normal Fabry-Perot oscillations. It is well known that in correspondence to

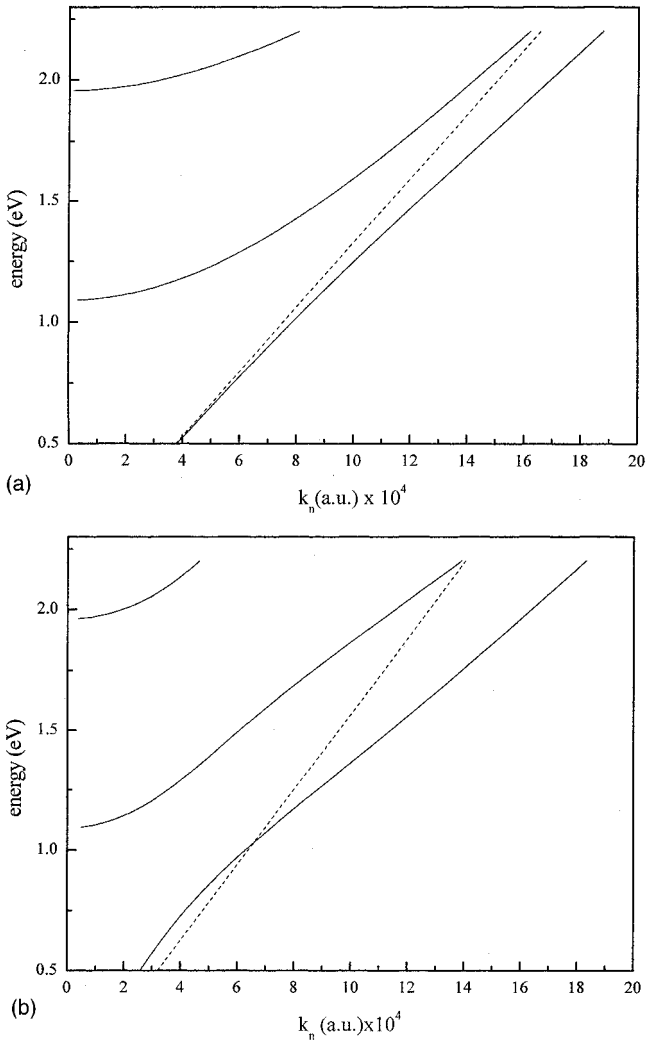

FIG. 4. Dispersion curves of the three lowest-energy eigenvalues of a rectangular dielectric grating for (a) *S* and (b) *P* polarizations (solid curves) for the same parameter values of Fig. 3.

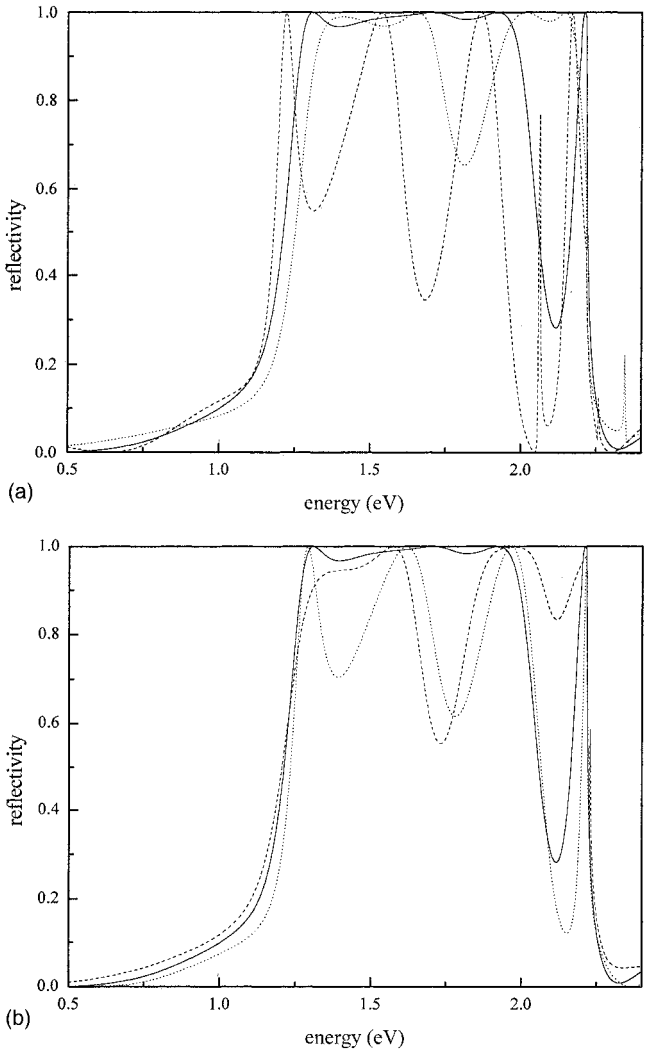

FIG. 5. *P*-polarization reflectivity for three values of (a) L_x (200-nm dotted curve, 225-nm solid curve, and 250-nm dashed curve) for $\Delta\epsilon=$const, and (b) the bulk dielectric constant (9.156 dotted curve, 10.156 solid curve, and 11.156 dashed curve) for $\overline{\epsilon}$ =const. The parameter values are given in the text.

these resonances the first propagating diffracted wave with high parallel-wave vector is confined (guided) to the grating region, and for direct and reflected waves in phase the reflectivity equal to 1 is reached.[5] For photon energy $\hbar\omega > E_2$ a second diffracted wave propagates in the structure, and therefore, the interference among three waves gives reflectivity with a line shape more and more complicated. In spite of this, the line shape is roughly composed by the Fabry-Perot oscillations of the equivalent slab with superimposed spikes due to the resonance conditions as assessed before [see Fig. 3(a)].

A rather different behavior is shown for *P*-polarization reflectivity as a function of photon energy [Fig. 3(b)]. In fact, a very low value of reflectivity $[|r_p(\omega)|^2 \leqslant 0.18]$ is observed for photon energy lower than the first threshold energy followed by a wide range of energy where reflectivity is rather one $[|r_p(\omega)|^2 \geqslant 0.97]$. Notice that this broad reflection band ($\Delta E = 0.85$ eV) is observed between the first and the second threshold energies of the diffracted waves as shown in Fig. 4(b). The low intensity of the Fabry-Perot oscillations ($G=0$) for *P* polarization is due to the incident angle chosen, that is very close to the Brewster angle ($\vartheta_B \approx 70°$) of the zero diffracted wave ($n=0$). This small reflectivity value increases the role in the optical response of the first diffracted wave ($n=1$) for energy $\hbar\omega > E_1$, and this property is of crucial importance in order to obtain sharp edge of the reflection band ($E_0 = 1.2$ eV).

The computed reflectivity spectra for *S* and *P* polarizations show a rather different behavior approaching the convergence ($N \to \infty$). While *S* polarization reflectivity for $N=3$ is just close to the spectrum at convergence, underlining the negligible contribution of the evanescent waves, for *P* polarization a strong contribution is observed. In fact, let us compare the three spectra of *P*-polarized reflectivity computed for $N=0$, 1 and at convergence ($N \to \infty$), respectively. Different behaviors are observed for three different ranges of energy, namely, (i) for $\hbar\omega < E_1$, the $N=1$ reflection curve shows Fabry-Perot oscillations similar to the equivalent slab

($N=0$), while this oscillations disappear at convergence, when also the contribution of the evanescent waves is taken into account. (ii) At higher energy ($E_1<\hbar\omega<E_2$) the $N=1$ reflection curve shows strong resonance peaks for $\hbar\omega$ values: 1.24, 1.58, and 1.96 eV. This set of resonances is due to the constructive interference between the normal wave ($n=0$) and the first diffracted wave ($n=1$) guided in the structure, and is obtained for selected values of the light wavelength respect to the periodicity and to the thickness of the grating.[5] At the convergence a crucial role in building up the reflection band is taken by evanescent surface waves that give very high reflectivity between adjacent resonant peaks [see Fig. 3(b)]. Therefore, this large reflection band is due to the interplay among traveling, guided, and evanescent waves in *P* polarization, and no simple qualitative evaluation is possible for describing this entangled phenomenon. (iii) For $\hbar\omega>E_2$ the second diffracted wave too becomes traveling in the structure, and the maximum of reflectivity for $\hbar\omega=2.21$ eV is not embodied in the reflection band because it is very close to the photon energy where the first diffracted wave escapes in the vacuum ($\hbar\omega\geqslant 2.2$ eV).

Finally, we want to point out that the general finding that in a multilayer system, embodying a dielectric grating, the convergence of the optical response calculation can be obtained by taking into account only the traveling and guided waves is incorrect.[13] Moreover, this polarization-sensitive reflection band is the most important result of our calculation, not only from fundamental point of view, but it should be also promising for the realization of large-band devices or it can be used as a mirror in the integrated all-optical circuits.

This mirror effect is very sensitive to the dielectric function values. In Figs. 5(a) and 5(b) the reflectivity spectra for different values of the diagonal ($\overline{\varepsilon}$) and of the out-of-diagonal ($\Delta\varepsilon$) matrix elements of the dielectric tensor, respectively, are computed by taking constant the periodicity and the thickness of the grating. In Fig. 5(a) we have reported the reflectivity for three different values of the lateral dimension of the wire, namely, L_x: 250, 225, and 200 nm. Notice that the dielectric contrast of the grating is taken constant ($\Delta\varepsilon=10.156$), and the reflection band worsen both increasing or decreasing the diagonal matrix element values with respect to the optimized one. In Fig. 5(b) the reflectivity is computed for three values of the dielectric contrast $\Delta\varepsilon$, obtained by changing the ε_b-values (namely, 12.156, 11.156, 10.156), and for L_x such that $\overline{\varepsilon}=8.617$. The out-of-diagonal matrix elements of the dielectric tensor are proportional to the dielectric contrast, that give the mixing among the different electromagnetic modes. Also, in this case a small variation of the $\Delta\varepsilon$ value worsen the reflection band line shape.

On the other hand, the mirror effect is rather stable with respect to the fluctuations of both the lateral dimension and thickness of the dielectric grating: in fact, it does not change appreciably for fluctuation within 3% for thickness and 2% for lateral dimension. Moreover, also the variation of the incident angle of the light does not affect the reflectivity band as we can see from Fig. 2, where for energy $\hbar\omega=1.4$ eV we observe reflectivity of about 1 for the range $45°\leqslant\vartheta_i\leqslant 75°$. For higher photon energy the grating Brewster angle value decreases (this feature is not reported here), giving a wider energy zone where the reflectivity is still one.

TABLE I. Reflectivity band energies for different grating parameters.

E_0 (eV)	ΔE (eV)	L_x (nm)	d (nm)	L_z (nm)	λ (nm)
1.80	1.32	150	200	240	235
1.20	0.85	225	300	350	352
0.90	0.64	300	400	470	469
0.45	0.33	600	800	960	938

It is well known that for coherence length of the light source much greater than the system thickness, the superposition of the plane waves is performed coherently, while if the coherence length is shorter, incoherent superposition should be done. In the latter case, by using the equivalence of thickness averaging and incoherent superposition,[16] the three resonances present in the reflectivity spectrum of Fig. 3(b) disappear, and analogously the broad-band effect. In our case the condition $L_c\gg L_z$ is easily satisfied for $L_c=\lambda^2/\Delta\lambda$, where $\Delta\lambda$ is the bandwidth of the laser, and therefore coherent superposition of plane waves can be adopted.

In Table I are reported the band energies computed by taking constant the incident angle of light and the dielectric contrast of the grating, while the values of L_z, L_x, and d are scaled according to the rules: (i) lateral dimension is scaled as $L_x/d=3/4$, and (ii) grating thickness $L_z\approx\lambda$, where λ is the light wavelength. In this case, while the reflectivity spectrum (not reported here) is similar to that shown in Fig. 3(b) the edge energy E_0 changes in a large range of values from infrared to ultraviolet. Moreover, for the grating with $d=300$ nm the reflectivity band is as large as all the visible energy range. Since the ratio $\Delta E/E_0\approx 3/4$ remains constant, and very close to L_x/d, the tailoring of this effect is due to the interplay between the Mie scattering of the light in the rectangular nanoparticle, and the multiscattering in the system with d periodicity. At variance with the photonic band gap phenomenon, where the internal electric field is stationary, in the present case the internal electric field is a guided wave and the vanishing surface waves take a key role in reflecting the incident electric field. Therefore, we guess that the name ''mirror effect'' does not generate confusion with photonic band gap and, on the other hand, is better connected with the physical surface origin of this phenomenon.[18]

IV. CONCLUSION

Green's functions for a grating with general nonlocal susceptibility are given, and their application to the optical response in the semi-infinite photonic crystals are briefly discussed.

Very broad reflection band in *P* polarization reflectivity at the Brewster angle is observed in a grating with strong dielectric contrast. This effect is due to (i) the resonance in the grating between normal and first-diffracted wave, and (ii) the contribution of the evanescent surface waves. Its easy tailor-

ing makes this phenomenon very promising for optical applications.

Finally, the validity of the generally used approximations, for the nonlocal optical response computation in gratings, is discussed.

ACKNOWLEDGMENTS

The authors are indebted to Professor R. Del Sole and Professor R. Bennaceur for useful discussions and to MADESS II Project for financial support.

[1] R. W. Wood, Philos. Mag. **4**, 396 (1902).
[2] E. Popov, L. Mashev and D. Maystre, Opt. Acta **32**, 607 (1986).
[3] S. S. Wang, R. Magnusson, J. S. Bagby and M. G. Moharam, J. Opt. Soc. Am. A **7**, 1464 (1990).
[4] L. Pilozzi, A. D'Andrea, and R. Del Sole, Phys. Rev. B **54**, 10 751 (1996).
[5] D. Rosenblatt, A. Sharon, and A. A. Friesem, IEEE J. Quantum Electron. **33**, 2038 (1997).
[6] Guy Levy-Yurista and Asher Friesem, Appl. Phys. Lett. **77**, 1596 (2000).
[7] M. Kohl, D. Heitmann, W. W. Ruhle, P. Grambow, and K. Ploog, Phys. Rev. B **41**, 12 338 (1990).
[8] M. Kohl, D. Heitmann, P. Grambow, and K. Ploog, Phys. Rev. B **42**, 2941 (1990).
[9] U. Bockelmann and G. Bastard, Phys. Rev. B **45**, 1688 (1992).
[10] A. D'Andrea and R. Del Sole, Phys. Rev. B **46**, 2363 (1992).
[11] L. Pilozzi, A. D'Andrea, and R. Del Sole, Phys. Rev. B **54**, 10 763 (1996).
[12] P. Ils, Ch. Greus, A. Forkel, V. D. Kulakovskii, N. A. Gippius, and S. G. Tikhodeev, Phys. Rev. B **51**, 4272 (1995).
[13] L. Pilozzi and A. D'Andrea, Phys. Rev. B **61**, 4771 (2000).
[14] A. K. Kavokin, M. A. Kliteevski, and M. R. Vladimirova, Phys. Rev. B **54**, 1490 (1996).
[15] A. Siarkos, E. Runge, and R. Zimmermann, Phys. Rev. B **61**, 10 854 (2000).
[16] Lifeng Li, Opt. Commun. **160**, 15 (1999).
[17] A. Bagchi, R. G. Barrera, and A. K. Rajagopal, Phys. Rev. B **20**, 4824 (1979).
[18] L. Pilozzi, N. Tomassini, and A. D'Andrea, in *Proceedings of 25th Conference on the Physics of Semiconductors, Osaka, Japan, September 17–22, 2000*, edited by N. Miura and T. Ando, SPP87 (Springer, Berlin, 2001).